

OPEN

# Sodium Hydrosulfide Treatment During Porcine Kidney Ex Vivo Perfusion and Transplantation

Thomas Agius, MS,<sup>1,2,3</sup> Julien Songeon, MS,<sup>4</sup> Arnaud Lyon, MD,<sup>1,5</sup> Justine Longchamp, MD,<sup>1</sup> Raphael Ruttimann, BS,<sup>6</sup> Florent Allagnat, PhD,<sup>1</sup> Sébastien Déglise, MD,<sup>1</sup> Jean-Marc Corpataux, MD,<sup>1</sup> Déla Golshayan, MD, PhD,<sup>5</sup> Léo Buhler, MD,<sup>7</sup> Raphael Meier, MD, PhD,<sup>8</sup> Heidi Yeh, MD,<sup>2,3</sup> James F. Markmann, MD, PhD,<sup>2,3</sup> Korkut Uygun, PhD,<sup>3</sup> Christian Toso, MD, PhD,<sup>6</sup> Antoine Klausner, PhD,<sup>4,9</sup> Francois Lazeyras, PhD,<sup>4,9</sup> and Alban Longchamp, MD, PhD<sup>1,2,3</sup>

**Background.** In rodents, hydrogen sulfide (H<sub>2</sub>S) reduces ischemia-reperfusion injury and improves renal graft function after transplantation. Here, we hypothesized that the benefits of H<sub>2</sub>S are conserved in pigs, a more clinically relevant model. **Methods.** Adult porcine kidneys retrieved immediately or after 60 min of warm ischemia (WI) were exposed to 100 μM sodium hydrosulfide (NaHS) (1) during the hypothermic ex vivo perfusion only, (2) during WI only, and (3) during both WI and ex vivo perfusion. Kidney perfusion was evaluated with dynamic contrast-enhanced MRI. MRI spectroscopy was further employed to assess energy metabolites including ATP. Renal biopsies were collected at various time points for histopathological analysis. **Results.** Perfusion for 4 h pig kidneys with Belzer MPS UW + NaHS resulted in similar renal perfusion and ATP levels than perfusion with UW alone. Similarly, no difference was observed when NaHS was administered in the renal artery before ischemia. After autotransplantation, no improvement in histologic lesions or cortical/medullary kidney perfusion was observed upon H<sub>2</sub>S administration. In addition, AMP and ATP levels were identical in both groups. **Conclusions.** In conclusion, treatment of porcine kidney grafts using NaHS did not result in a significant reduction of ischemia-reperfusion injury or improvement of kidney metabolism. Future studies will need to define the benefits of H<sub>2</sub>S in human, possibly using other molecules as H<sub>2</sub>S donors.

(*Transplantation Direct* 2023;9: e1508; doi: 10.1097/TXD.0000000000001508.)

One of the challenges in solid organ transplantation is improving the organ preservation method especially in the grafts with inferior quality. The current clinical standard for kidney preservation is hypothermic preservation/perfusion at +4°C for a typical storage duration of ~20 h. Hypothermic nonoxygenated preservation results in a slow but inexorable deterioration of vital cellular functions, notably ATP

production and redox homeostasis, eventually leading to cell death. Hypothermic machine perfusion (HMP) has been developed as an alternative preservation method to static cold storage (SCS) with promising short-term results.<sup>1</sup> In a landmark study including 672 kidney transplant recipients, HMP reduced ischemia-reperfusion injury, clinically manifested as delayed graft function.<sup>2</sup> These results were confirmed by later

Received 14 April 2023. Revision received 1 May 2023.

Accepted 16 May 2023.

<sup>1</sup> Department of Vascular Surgery, Lausanne University Hospital, Lausanne, Switzerland.

<sup>2</sup> Department of Surgery, Transplant Center, Massachusetts General Hospital, Harvard Medical School, Boston, MA.

<sup>3</sup> Department of Surgery, Center for Engineering in Medicine, Massachusetts General Hospital, Harvard Medical School, Boston, MA.

<sup>4</sup> Department of Radiology and Medical Informatics, University of Geneva, Geneva, Switzerland.

<sup>5</sup> Department of Medicine, Transplantation Centre, Lausanne University Hospital, Lausanne, Switzerland.

<sup>6</sup> Visceral and Transplant Surgery, Department of Surgery, Geneva University Hospitals and Medical School, Geneva, Switzerland.

<sup>7</sup> Section of Medicine, Faculty of Science and Medicine, University of Fribourg, Switzerland.

<sup>8</sup> Department of Surgery, University of Maryland School of Medicine, Baltimore, MD.

<sup>9</sup> CIBM Center for Biomedical Imaging, Geneva, Switzerland.

The authors declare no conflicts of interest.

Supported by the Swiss National Science Foundation to J.M.C., FL (SNSF 320030\_182658), and AL (SNSF PZ00P3-185927) as well as the Mendez National Institute of Transplantation, and the Mercier Foundation to AL.

T.A., J.S., F.A., S.D., J.M.C., L.B., R.M., K.U., C.T., A.K., F.L., and A.L. participated in research design. T.A., J.S., Ar.L., J.L., R.R., F.A., S.D., J.M.C., D.G., L.B., R.M., H.Y., J.F.M., K.U., C.T., A.K., F.L., and A.L. participated in the writing of the article. T.A., J.S., Ar.L., J.L., R.R., J.M.C., R.M., A.K., F.L., and A.L. participated in the performance of the research. T.A., J.S., Ar.L., J.L., F.L., and A.L. participated in data analysis.

Correspondence: Alban Longchamp, MD, PhD, Division of Transplantation, Massachusetts General Hospital, Mass General Brigham, 55 Fruit Street, Boston, MA 02114. (alongchamp@mgh.harvard.edu).

Copyright © 2023 The Author(s). *Transplantation Direct*. Published by Wolters Kluwer Health, Inc. This is an open-access article distributed under the terms of the Creative Commons Attribution-Non Commercial-No Derivatives License 4.0 (CCBY-NC-ND), where it is permissible to download and share the work provided it is properly cited. The work cannot be changed in any way or used commercially without permission from the journal.

ISSN: 2373-8731

DOI: 10.1097/TXD.0000000000001508

meta-analysis, demonstrating that HMP reduces the incidence of delayed graft function in all types of donors: standard and extended criteria donors, in both donation after brainstem and donation after circulatory death (DCD).<sup>1</sup>

Hydrogen sulfide (H<sub>2</sub>S) is a small endogenous gaseous molecule produced mainly by cystathionine gamma-lyase or cystathionine beta-synthase.<sup>3,4</sup> During ischemia-reperfusion injury, genetic deletion of cystathionine gamma-lyase was shown to increase damage and mortality after renal ischemia-reperfusion injury in mice, which could be rescued by exogenous H<sub>2</sub>S sodium hydrosulfide (NaHS).<sup>5</sup> Similarly, we demonstrated that administration of exogenous NaHS in wild-type mice reduced hepatic and renal ischemia-reperfusion injury.<sup>6</sup> Addition of NaHS to Belzer MPS UW preservation solution in SCS reduced necrosis apoptosis and improved early kidney function after transplantation in rats.<sup>7</sup> In porcine kidneys subjected to 2 h of warm ischemia (WI), administration of H<sub>2</sub>S systemically or into the renal artery before reperfusion improved creatine clearance, reduced apoptosis, and tubular injury.<sup>8</sup> Moreover, the addition of AP39 (a mitochondrial-targeted H<sub>2</sub>S donor) during porcine kidneys subnormothermic perfusion (21°C) for 4 h with an O<sub>2</sub> carrier (Hemopure) improved urine output and graft oxygenation.<sup>9</sup>

Relevant to ischemia-reperfusion injury, H<sub>2</sub>S was shown to have direct antioxidant properties,<sup>10</sup> can promote glutathione synthesis and induced stress response pathways (eg, Nrf2).<sup>11</sup> Of importance, we previously demonstrated that H<sub>2</sub>S can reversibly inhibit the mitochondrial electron transport chain, thus reducing reactive oxygen species (ROS) formation during reperfusion.<sup>3,12</sup> In ischemic conditions, H<sub>2</sub>S promotes glucose uptake and glycolytic ATP production.<sup>3</sup> The ATP depletion occurring during ischemia causes inhibition of mitochondrial Na<sup>+</sup>/K<sup>+</sup> ion channels, resulting in increased mitochondrial inner membrane permeability and cell death. In prior studies, we used MRI, and <sup>31</sup>P magnetic resonance spectroscopic imaging (pMRSI) for the detection of high-energy phosphate metabolites such as ATP during kidney transplantation.<sup>13</sup> In fact, recovery from ischemia-reperfusion injury is an ATP-dependent process,<sup>14</sup> and ATP level was shown to determine kidney graft function following transplantation.<sup>13</sup>

Here, using MRI and pMRSI, we examined the effect of exogenous H<sub>2</sub>S (NaHS) in a relevant porcine ex vivo HMP model and autotransplantation. The effect of H<sub>2</sub>S was evaluated in both kidneys that were retrieved immediately, as well as after 60 min of WI to mimic circulatory arrest during DCD procurement. To increase the translational value of our study, NaHS was given in relevant clinical situations, including ex vivo perfusion only, or concomitant to heparin administration before WI.

## MATERIAL AND METHODS

### Animals and Surgery

The study was approved by the University of Geneva's animal ethics committee (protocol number: GE83/33556). Five-month-old female pigs were obtained from the animal facility of Arare, Switzerland. All pigs were maintained under standard conditions. Water and food were provided ad libitum. Animals were premedicated, anesthetized then kept intubated and ventilated during the procedure.<sup>15</sup> An arterial line was inserted in the internal carotid artery. Monitoring included heart rate, systemic blood pressure, pulse oximetry, and end-tidal CO<sub>2</sub>. All surgeries were performed by the same surgeon. After a

midline incision, the peritoneal cavity was opened, and the bowels were retracted. Abdominal aorta, inferior vena cava, and renal vessels were dissected. The pigs received 300 IU/kg heparin intravenously. In some groups, 1 ml of 100 μM NaHS was administered into the renal artery 10 min before clamping. The kidneys were either immediately explanted or after 60 min of WI (DCD model). During the WI, the arterial inflow was interrupted using an atraumatic clamp. Blood flow cessation was verified using a handheld Doppler. The model did not include an agonal phase. Kidneys were then instantly flushed with 1 L of Belzer MPS UW Machine Perfusion Solution on ice with or without 100 μM NaHS. The renal artery was cannulated, and the kidneys were perfused for 3 h (see later), as previously described using our MRI-compatible machine.<sup>13,16</sup> At the end of the perfusion, both kidneys were transplanted sequentially with anastomosis on the inferior vena cava and infrarenal aorta using a prolene 6-0 running suture. Of importance, the implantation of 2 kidneys in the same recipient precluded any blood-based analysis of kidney function. After 2 h of in vivo reperfusion, pigs were sacrificed using 100 mEq of potassium chloride intravenously.

### Ex Vivo Kidney Perfusion

Flushed kidneys were perfused for a total of 4 h (3 h before the MRI, 45 min during the MRI, and 15 min transport to the MRI, see later) with Belzer MPS UW Machine Perfusion Solution in presence or absence of 100 μM NaHS (as indicated in the figures and legends), active oxygenation was achieved using a 0.15 m<sup>2</sup> membrane oxygenator (Biochrom Ltd, Cambridge, UK), maintaining the pO<sub>2</sub> levels at 100 kPa for the whole preservation time, and measured every 30 min with a blood gas analyzer. The perfusion module was kept in an insulating box containing ice keeping the kidney at 4°C. Systolic and diastolic pressure were set at 40 and 20 mm Hg, respectively.

### MRI

MRI and pMRSI (see later) were performed during the ex vivo perfusion pretransplantation, and posttransplantation, as indicated in the figures and legends. Measurements were performed on a 3 Tesla multi-nuclear Prisma-fit 3T whole-body MRI scanner (Siemens Healthineers, Erlangen, Germany). <sup>1</sup>H imaging was performed with the body coil using a T2-weighted sequence (turbo spin echo, repetition time 6530 ms, echo time 110 ms, 2 mm slices) for kidney localization and structural imaging. Dynamic contrast-enhanced MRI with gadolinium was used to determine the perfusion distribution between the cortex and the medulla, a surrogate of glomerular filtration rate as previously described.<sup>13,16</sup> Data were collected using a dynamic 2-dimensional sequence with the scanner body coil. This sequence has an inversion time of 255 ms, a flip angle of 12°, 1.3 mm × 1.3 mm resolution, 6 slices of 4 mm (1 mm gap), repetition time 500 ms, and an echo time of 1.4 ms. The perfusion-descending cortical slope was determined for the cortex and the medulla using the angle of the linear regression between the maximum signal value and the lowest intensity point after the initial peak.<sup>13</sup>

### PMRS Imaging

pMRSI was performed as described previously.<sup>13,16,17</sup> Briefly, a single-loop <sup>31</sup>P-tuned coil fixed at the bottom of the perfusion tank allows the measurement of the signal. Scanner embedded body coil was used for <sup>1</sup>H imaging and for shimming to ensure

field homogeneity. pMRSI consisted of 3-dimensional spatial encoding, with a field-of-view  $250 \times 250 \times 160 \text{ mm}^3$ , matrix size  $16 \times 16 \times 8$ , nominal spatial resolution  $15.6 \times 15.6 \times 20 \text{ mm}^3$ , repetition time 1.0s, flip angle 35 degrees, echo delay 0.6ms, bandwidth 4000 Hz, 2 k sampling points. Elliptical encoding with 18 weighted averages resulted in an acquisition time of 45 min. The resonance of the inorganic phosphate (Pi, 5.2 ppm), which is uniformly present in the container and the kidney, was used as a reference for quantification of the pMRSI signal. Excitation pulse bandwidth has been adjusted to the ATP frequency range (Pi resonance—500 Hz). An exponential time filter (apodization) with 20 Hz bandwidth, zeroth, and first-order phase corrections were used to process the spectra. The metabolites (ATP, phosphomonoesters, Pi, phosphocreatine) were fitted with Gaussian peaks using the syngo.via software (SIEMENS, Erlangen, Germany) and were estimated over the whole kidneys by averaging pMRSI voxels containing graft tissue, resulting in a single spectrum. The 3 ATP peaks were quantified separately to prevent methodological bias because of excitation profile imperfection. In each condition, pMRSI allowed the detection of Alpha ( $\alpha$ )-, beta ( $\beta$ )-, and gamma ( $\gamma$ )-ATP and phosphomonoesters composed of phosphocholine, phosphoethanolamine, and AMP. ATP and phosphomonoesters concentration (mM) were calculated using a known concentration of the Pi (25 mM) as reference<sup>13</sup> because single ATP concentration was calculated by average of the  $\alpha$ -,  $\beta$ -, and  $\gamma$ -ATP values.

### Histopathological Analysis of Biopsies

Surgical kidney cortical biopsies were collected at baseline (before clamping), after WI, at the end of the ex vivo perfusion (pretransplantation), and after 2 h of reperfusion/transplantation (posttransplantation), which were formalin-fixed then embedded in paraffin. Fixed kidney biopsies were cut into sections of 3  $\mu\text{m}$  thickness and stained with silver Jones and periodic acid-Schiff. Slides were scanned using an Axio Scan z1 slide scanner (Zeiss). The histopathological analysis score was performed based on those described by Goujon et al<sup>16,18,19</sup> using Zen software (Zeiss) and previously demonstrated to reflect the degree of injury posttransplantation.<sup>13,16</sup> Whole biopsies were assessed and blinded to group assignment. The following categories were assessed: glomerular integrity, tubular dilatation, tubular brush border integrity, cellular debris in the lumen of tubules, interstitial edema, and tubular cell vacuolization. Each category was assigned a score of 0–3 (low to high degree of injury), which was then converted to a percentage of damage. This was converted to a final scale from 0 to 5 according to the percentage of damage: 0%–15% (0), 15%–30% (1), 30%–45% (2), 45%–60% (3), 60%–75% (4), and >75% (5) using the following formula:  $(\text{Category}_{\text{Final Score}}/3) * 100$ . The final score for each biopsy ranged from 0 to 30 with 30 the highest score corresponding to more severe damage. Scoring was performed blindly by 2 independent researchers.

### Statistical Analysis

Data are presented as mean  $\pm$  SEM, and differences are considered significant when  $P < 0.05$ . Comparisons between groups were analyzed using analysis of variance and post hoc Tukey tests. Two-group comparisons were performed using Student t tests (Prism 9.2, GraphPad Softwares, San Diego,

CA). Fitting curves of the concentration of metabolites over time were computed using R (4.1, <https://cran.r-project.org>).

## RESULTS

### H<sub>2</sub>S Treatment During HMP

We first examined the effect of H<sub>2</sub>S administration during ex vivo perfusion (Figure 1A). Immediately after harvest, kidneys were flushed and perfused with 4°C Belzer MPS UW solution with or without (control) 100  $\mu\text{M}$  NaHS before autotransplantation. After 3 h of cold perfusion, cortical and medullary flow were similar in both the control- and the NaHS-treated kidneys (Figure 1B). This was reflected by the absence of significant differences in the perfusion-descending cortical slope ( $-78 \pm 1.32$  and  $P = 0.53$  cortex,  $-67 \pm 14.8$ ;  $P = 0.10$  medulla for control and NaHS, respectively, Figure 1B). Next, mean ATP levels were measured by averaging pMRSI voxels containing graft tissue.<sup>13,16</sup> Alpha ( $\alpha$ ), beta ( $\beta$ ), and gamma ( $\gamma$ ) ATP, and phosphomonoesters containing AMP, were similar in both groups (Figure 1C). Similarly, post-autotransplantation, cortical and medullary flow (Figure 1D), and ATP levels (Figure 1E) were similar in both control- and NaHS-treated kidneys. Finally, we examined the histologic damage using a modified Goujon score (described in the methods section), shown to reflect kidney function.<sup>13,16,18</sup> Kidney biopsies were analyzed at baseline, at the end of the ex vivo perfusion (pretransplantation), and 2 h posttransplantation. Consistent with previous findings, histologic damages, were significantly increased after transplantation/ reperfusion (Figure 1F). It is important to note that treatment with NaHS during ex vivo perfusion did not reduce histologic injuries, such as tubular dilatation, luminal cell debris, and brush border lesions before and after transplantation (Figure 1F).

### H<sub>2</sub>S Treatment During HMP in DCD Grafts

Because we did not observe any benefits of H<sub>2</sub>S treatment in organs retrieved immediately, we next investigated the effect of NaHS in kidneys obtained after 60 min of WI. Immediately after procurement, kidneys were flushed and perfused for 3 h with 4°C Belzer MPS UW solution with 100  $\mu\text{M}$  NaHS or vehicle (control) before autotransplantation (Figure 2A). In DCD kidneys, at the end of 4°C ex vivo perfusion, cortical and medullary flow were similar in both the control- and the NaHS-treated kidneys (Figure 2B). Similarly, at the end of ex vivo perfusion, ATP levels were unaffected by NaHS administration (Figure 2C). In addition, after transplantation, kidney perfusion (Figure 2D), ATP levels (Figure 2E), and histologic injuries (Figure 2F) were not reduced by the administration of NaHS during the ex vivo perfusion.

### H<sub>2</sub>S Treatment Before Ischemia in DCD

The absence of significant differences observed between the control- and H<sub>2</sub>S-treated DCD kidneys might be related to the timing of NaHS administration. Thus, we investigated the effect of a single injection of 100  $\mu\text{M}$  NaHS, directly into the renal artery before the interruption of blood flow (WI, Figure 3A). In these conditions, kidney perfusion and descending slopes were similar in both the control and NaHS-treated kidney (Figure 3B) during ex vivo perfusion. Similarly, intra-arterial NaHS administration before ischemia did not impact ATP production in perfused kidneys (Figure 3C). After transplantation, cortical and medullary perfusion were similar in

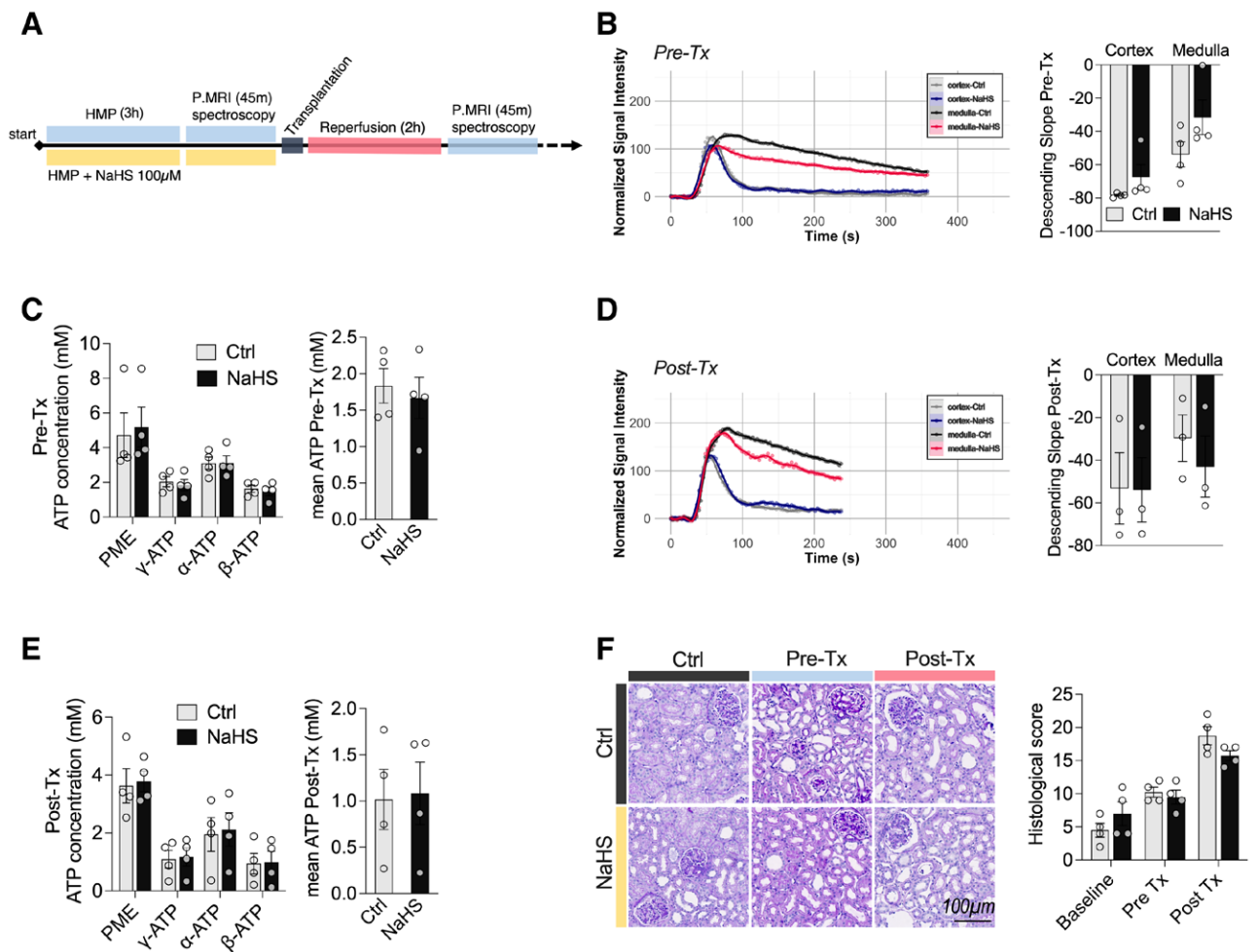


**FIGURE 1.** Effects of  $H_2S$  supplementation during HMP. (A) Experimental design. Pig kidneys were perfused at  $4^\circ C$  with  $O_2$  (HMP) with Belzer MPS UW with or without  $100 \mu M$  NaHS for 3h, during  $^{31}P$  MRSI and before autotransplantation (reperfusion) and posttransplant  $^{31}P$  MRSI during  $^{31}P$  MRSI and before autotransplantation (reperfusion) and posttransplant  $^{31}P$  MRSI (B) Pretransplant cortical and medullary Gd-normalized signal intensity over time (right) and quantification (descending slopes, left) in the indicated groups. (C) Pretransplant phosphomonoesters,  $\alpha$ ,  $\beta$ , and  $\gamma$  ATP levels (left) and mean ATP (right) in control- and NaHS-treated kidney. (D) Posttransplant cortical and medullary Gd-normalized signal intensity over time (right) and quantification (descending slopes, left) in the indicated groups. (E) Posttransplant phosphomonoesters,  $\alpha$ ,  $\beta$ , and  $\gamma$  ATP levels (left) and mean ATP (right) in control- and NaHS-treated kidney. (F) Representative transverse PAS-stained sections of kidneys at the indicated time in control and NaHS groups (left) and quantification of histologic damages (score, right). Data expressed as mean  $\pm$  SEM,  $n = 4$ . ATP; Gd, gadolinium; HMP, hypothermic machine perfusion;  $H_2S$ , hydrogen sulfide; MPS UW, sodium hydrosulfide; PAS, periodic acid-Schiff; PME, phosphomononucleotide; PMRSI,  $^{31}P$  magnetic resonance spectroscopic imaging; Tx, transplantation.

both groups (Figure 3D). Similarly, we did not observe differences in ATP concentration (Figure 3E) or histologic injuries (Figure 3F).

We reasoned that a single injection of NaHS before WI might be insufficient because of uncontrolled rapid delivery of  $H_2S$  observed with NaHS. Therefore,  $100 \mu M$  NaHS was administered into the renal artery, before WI as well as in the perfusate, during the entire ex vivo perfusion period (Figure 4A). Under this condition, cortical and medullary perfusion after transplantation were similar in the vehicle and NaHS-treated kidney (Figure 4B).  $\alpha$ ,  $\beta$ , and  $\gamma$  ATP, and phosphomonoesters containing AMP, were similar in both groups (Figure 4C). Finally, using the Goujon score, we did not detect significant differences in histologic damages in both groups (Figure 4D).

## DISCUSSION

In this study, we found that  $100 \mu M$  NaHS administration during ex vivo kidney perfusion in kidney porcine graft,

and before WI in a DCD model, did not improve energy metabolism, kidney perfusion, or histologic damages upon transplantation.

Our group and others previously demonstrated that NaHS protects against renal ischemia-reperfusion injury in several models of warm tissue ischemia, as well as during cold preservation before transplantation in rodents.<sup>3,6,8,20</sup> However, we could not replicate these findings here in an adult pig model (approximately animal weight 35 kg) during cold storage followed by in vivo reperfusion/transplantation. Of interest, in mice, exposure to 20–80 ppm gaseous  $H_2S$  dose-dependently decreased energy expenditure within a few minutes, as assessed by whole-body  $O_2$  uptake and  $CO_2$  production. This fall in metabolic activity was associated with bradypnea and consecutive hypothermia, with core temperature falling to levels close to ambient values.<sup>21</sup> Subsequent work has thus described and studied  $H_2S$ -induced suspended animation—a hibernation-like state. Various other rodent models confirmed these observations: Inhaling gaseous  $H_2S$ <sup>22</sup> and

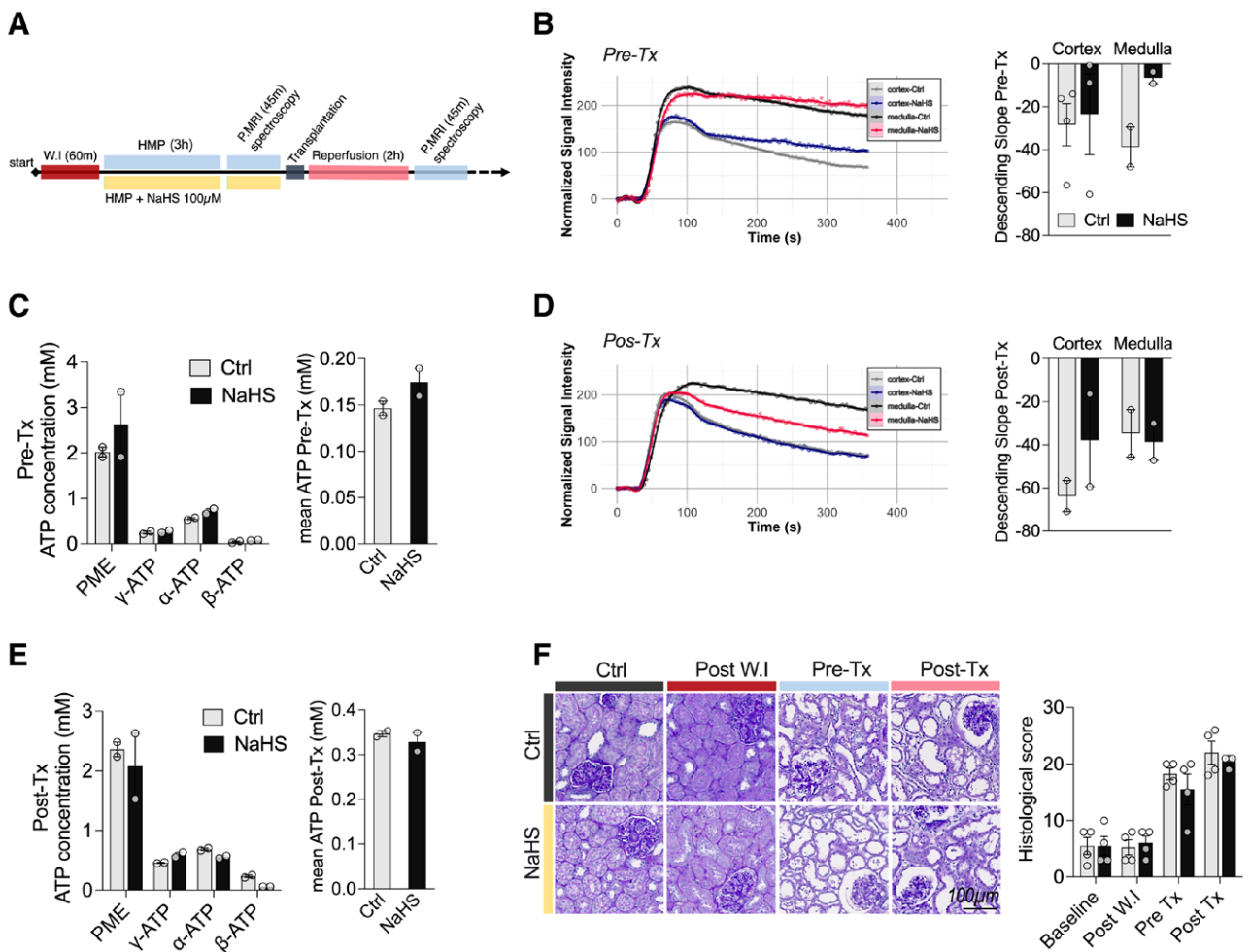


**FIGURE 2.** Effects of  $H_2S$  supplementation during HMP in a DCD model. (A) Experimental design. Pig kidneys underwent 60 min of WI before  $4^\circ C$  oxygenated (HMP) with Belzer MPS UW with or without  $100 \mu M$  NaHS for 3 h during  $^{31}P$  MRSI and before autotransplantation (reperfusion) and posttransplant  $^{31}P$  MRSI assessment. (B) Pretransplant cortical and medullar Gd-normalized signal intensity over time (right) and quantification (descending slopes, left) in the indicated groups. (C) Pretransplant phosphomonoesters,  $\alpha$ ,  $\beta$ , and  $\gamma$  ATP levels (left) and mean ATP (right) in control- and NaHS-treated kidney. (D) Posttransplant cortical and medullar Gd-normalized signal intensity over time (right) and quantification (descending slopes, left) in the indicated groups. (E) Posttransplant phosphomonoesters,  $\alpha$ ,  $\beta$ , and  $\gamma$  ATP levels (left) and mean ATP (right) in control- and NaHS-treated kidney. (F) Representative transverse PAS-stained sections of kidneys at the indicated time in control and NaHS groups (left) and quantification of histologic damages (score, right). Data expressed as mean  $\pm$  SEM,  $n = 3$ . ATP; DCD, donation after circulatory death; HMP, hypothermic machine perfusion;  $H_2S$ , hydrogen sulfide; MPS UW, NaHS, sodium hydrosulfide; PAS, periodic acid-Schiff; PME, phosphomononucleotide; PMRSI,  $^{31}P$  magnetic resonance spectroscopic imaging; Tx, transplantation; WI, warm ischemia.

infusing the soluble sulfide salts ( $NaHS$  or  $Na_2S$ )  $Na_2S$  also induced a reversible reduction in energy expenditure with a subsequent fall in core temperature.<sup>23</sup> Of utmost importance, the metabolic depressant property of  $H_2S$  appears to depend on the animal size. In rats, the  $H_2S$ -induced decrease in  $O_2$  uptake was several-fold lower than in mice.<sup>24</sup> In larger species (swine, sheep), various authors failed to confirm any  $H_2S$ -related reduction in metabolic activity at all, regardless of the administration route.<sup>25</sup> Similarly, in sheep, gaseous  $H_2S$  administration had no impact on whole-body  $O_2$  uptake,  $CO_2$  production, and cardiac output.<sup>26</sup> The reduction in oxygen consumption induced by  $H_2S$  is thought to occur via reversible inhibition of the mitochondrial electron transport complex I and IV.<sup>3</sup> Upon reperfusion, the accumulated succinate is rapidly re-oxidized, driving extensive ROS generation by reverse electron transport at mitochondrial complex I.<sup>27</sup> It is important to note that it remained to be tested if the inhibition of complex I is required to protect from ischemia-reperfusion injury upon  $H_2S$  exposure. However, these data are consistent

with our latest findings and suggest that achieving metabolic suppression (suspended animation-like status), and subsequent protection from WI and cold ischemia in larger animals, or humans will be more difficult and would require more time because of the small surface area/mass ratio.<sup>28</sup> Alternatively,  $H_2S$  can directly scavenge ROS, or at more relevant physiological concentration can stimulate antioxidant pathways (such as glutathione via the transsulfuration pathways).<sup>10</sup>

$NaHS$  dissociates to  $Na^+$  and  $HS^-$  and then binds partially to  $H^+$  to form undissociated  $H_2S$ . Although  $H_2S$  levels were not measured in this study,  $NaHS$  rapidly releases  $H_2S$ , the effect occurring within seconds.<sup>3</sup> Thus,  $NaHS$  rapid and uncontrolled delivery of  $H_2S$  might contribute to the absence of effect observed in this study. Diallyl trisulfide and diallyl disulfide are other  $H_2S$ -releasing molecules that protect from ischemia-reperfusion injury but are also unstable and short-lived.<sup>29</sup> Morpholin-4-ium-4-methoxyphenyl phosphinodithioate (GYY4137) might be a more attractive alternative, as it releases  $H_2S$  at a slow and steady rate at physiological pH

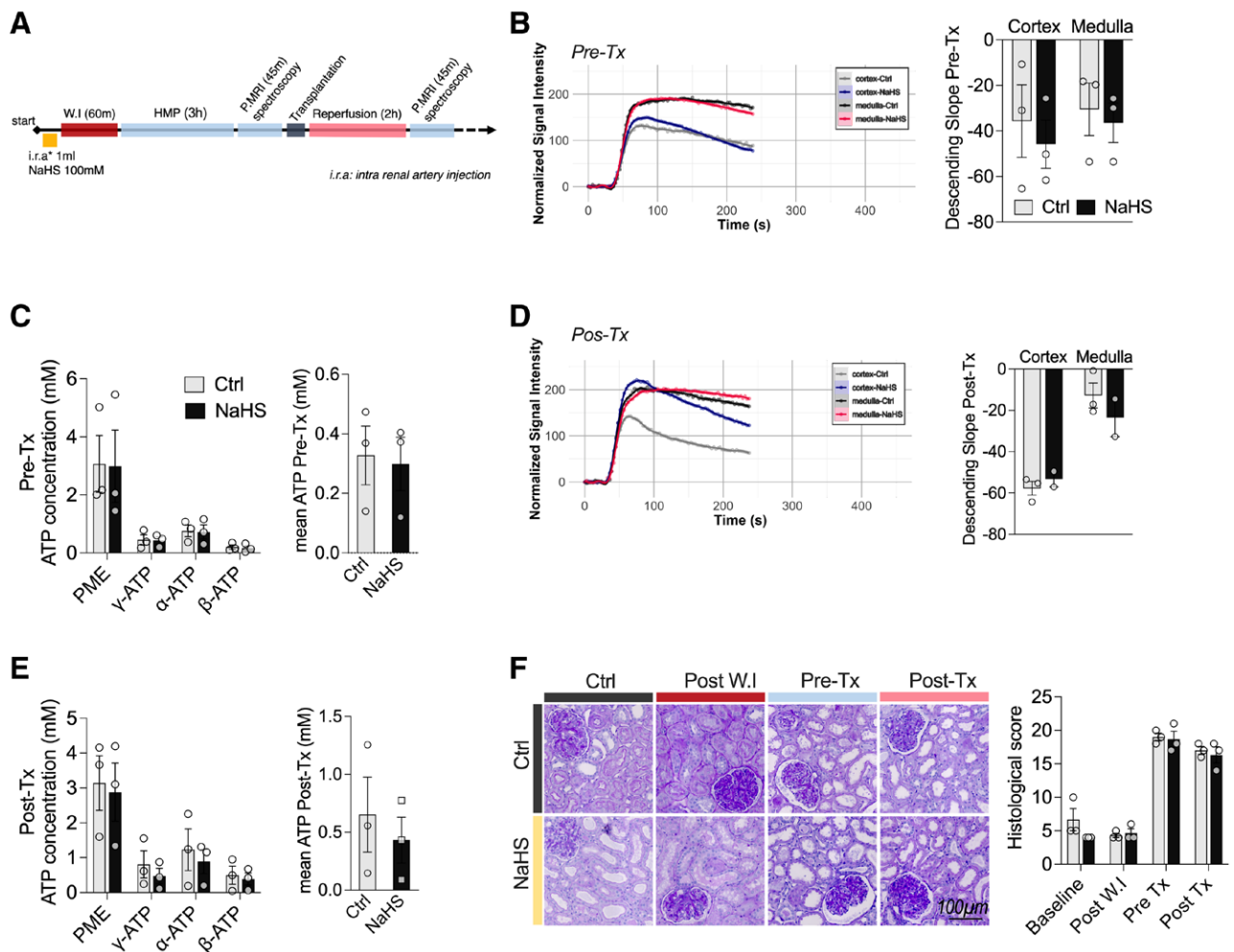


**FIGURE 3.** Administration of  $H_2S$  before WI in a DCD model. (A) Experimental design: Administration of 100  $\mu M$  NaHS into the renal artery before 60 min WI. Immediately after procurement, kidneys were perfused at  $4^\circ C$  with  $O_2$ , in Belzer MPSJ UW for 3 h and underwent  $^{31}P$  MRSI, before autotransplantation (reperfusion) and posttransplant  $^{31}P$  MRSI assessment. (B) Pretransplant cortical and medullar Gd-normalized signal intensity over time (right) and quantification (descending slopes, left) in the indicated groups. (C) Pretransplant phosphomonoesters,  $\alpha$ ,  $\beta$ , and  $\gamma$  ATP levels (left) and mean ATP (right) in control- and NaHS-treated kidney. (D) Posttransplant cortical and medullar Gd-normalized signal intensity over time (right) and quantification (descending slopes, left) in the indicated groups. (E) Posttransplant phosphomonoesters,  $\alpha$ ,  $\beta$ , and  $\gamma$  ATP levels (left) and mean ATP (right) in control- and NaHS-treated kidney. (F) Representative transverse PAS-stained sections of kidneys at the indicated time in control and NaHS groups (left) and quantification of histologic damages (score, right). Data expressed as mean  $\pm$  SEM,  $n = 3$ . ATP, DCD, donation after circulatory death; Gd, gadolinium;  $H_2S$ , hydrogen sulfide; MPSJ UW, NaHS, sodium hydrosulfide; PAS, periodic acid-Schiff; PME, phosphomononucleotide; PMRSI,  $^{31}P$  magnetic resonance spectroscopic imaging; Tx, transplantation; WI, warm ischemia.

and temperature.<sup>30</sup> GYY4137 was shown to mitigate renal acute kidney injury following ischemia-reperfusion in mice.<sup>31</sup> In vitro, the mitochondrial-targeted  $H_2S$  prodrug AP39 was shown to be significantly more potent than GYY4137. In rats, AP39 improved renal allograft survival following 24 h SCS and transplantation.<sup>32</sup> In DCD porcine kidneys, ex vivo subnormothermic perfusion (SNMP,  $21^\circ C$ ) with autologous blood and AP39 improved urine output and reduced apoptosis compared with SCS or SNMP alone for 4 h.<sup>9</sup> Of note, reperfusion was assessed ex vivo with autologous blood at  $37^\circ C$ , and the kidneys were not transplanted in the latter study.<sup>9</sup> It is important to note that these  $H_2S$  donors remain to be tested in larger animals during cold preservation, which remains the easiest and most employed method during kidney preservation.

We did not compare the effect of NaHS at higher perfusion temperatures (SNMP at  $21^\circ C$  or NMP at  $37^\circ C$ ). (S)NMP provides a continuous flow of warmed, oxygenated perfusate containing nutritional substrates, aiming to maintain the metabolic activity of the kidney.<sup>33</sup> Instead, the rationale here was

to use  $H_2S$ -specific inhibition of the mitochondrial electron transport chain during cold preservation and reduce ROS generation during reperfusion, rather than solely relying on passive temperature effects to depress metabolism.<sup>3</sup>

ATP measurement relied exclusively on pMRSI. However, we previously demonstrated that nucleotide quantification with pMRSI was accurate.<sup>16</sup> pMRSI also suffers from a relatively low sensitivity compared with liquid chromatography or  $^1H$  imaging at a constant magnetic field.<sup>13</sup> Thus, the acquisition is generally performed with a higher voxel size to achieve enough signal-to-noise ratio while keeping an acceptable scan time. Of importance, this lack of sensitivity limitation hinders the measurement of ATP at  $4^\circ C$  without oxygen. The application of machine learning and neural network can further improve pMRSI sensitivity, spatial resolution, and computing time.<sup>34,35</sup> Overall pMRSI remains a powerful, noninvasive tool to quantify ATP.<sup>13</sup>

Our study has several limitations that need to be acknowledged. Kidney function (serum creatinine, urea, and estimated glomerular filtration rate) and urine production after

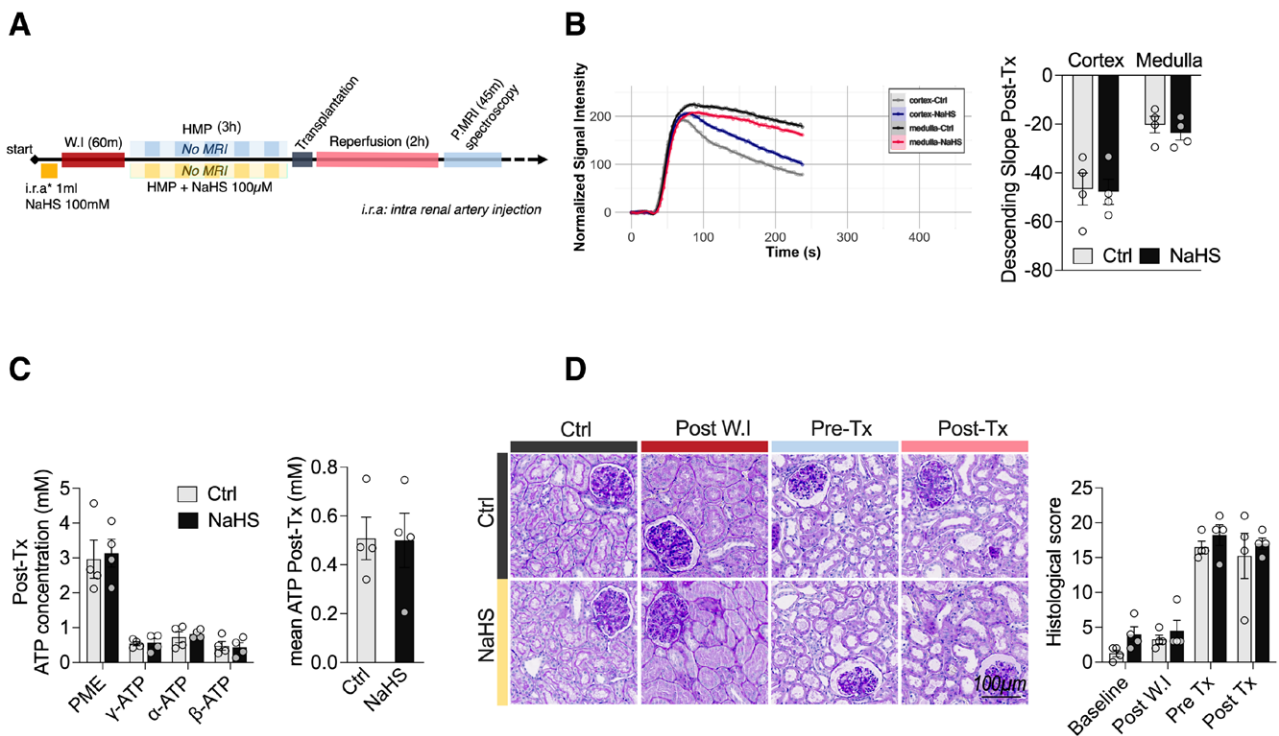


**FIGURE 4.** Administration of H<sub>2</sub>S before WI and during HMP in a DCD model. (A) Experimental design. Administration of 100 μM NaHS into the renal artery before 60min WI. Immediately after procurement, kidneys were perfused at 4°C without O<sub>2</sub>, in Belzer MPS UW with or without NaHS as indicated for 3h, before autotransplantation (reperfusion) and posttransplant <sup>31</sup>P MRSI assessment. (B) Posttransplant cortical and medullary Gd-normalized signal intensity over time (right) and quantification (descending slopes, left) in the indicated groups. (C) Posttransplant phosphomonoesters, α, β, and γ ATP levels (left) and mean ATP (right) in control- and NaHS-treated kidney. (D) Representative transverse PAS-stained sections of kidneys at the indicated time in control and NaHS groups (left) and quantification of histologic damages (score, right). Data expressed as mean ± SEM, n = 4. ATP; DCD, donation after circulatory death; Gd, gadolinium; HMP, hypothermic machine perfusion; H<sub>2</sub>S, hydrogen sulfide; MPS UW; NaHS, sodium hydrosulfide; PAS, periodic acid-Schiff; PME, phosphomononucleotide; PMRSI, <sup>31</sup>P magnetic resonance spectroscopic imaging; Tx, transplantation; WI, warm ischemia.

transplantation were not assessed. Kidney function tests could not be performed because of local regulations, which did not allow survival surgery. In addition, follow-up beyond 2h after transplantation would be required to truly assess longer-term graft injury and function. Thus, the histologic score, previously correlated with the degree of kidney injury was used as a surrogate endpoint of kidney function.<sup>13,15,18,19</sup> Similarly, the sample size was small, thus increasing the risk of type II errors. As discussed earlier, other H<sub>2</sub>S-releasing molecules or gaseous H<sub>2</sub>S should be evaluated in the (pre)clinical model of kidney transplantation. In addition, our study only included healthy adult pig kidneys. Similar studies should be performed using marginal (eg, old) kidney grafts.

In conclusion, perfusion of porcine kidneys with NaHS did not improve preservation nor reduced ischemia-reperfusion injury. Perfusion of organs with alternative H<sub>2</sub>S donors, or at different temperatures should be tested to determine if H<sub>2</sub>S can improve posttransplant graft function and patient survival.

## ACKNOWLEDGMENTS

The authors thank Jean-Pierre Giliberto from the Department of Surgery, University Hospitals of Geneva for the excellent technical assistance. They thank the cellular imaging facility for access and training on the ZEISS Axioscan 7 Microscope Slide Scanner (<https://cif.unil.ch>). They thank the mouse pathology facility for assistance with paraffin

embedding and cutting of the tissues (<https://www.unil.ch/mpf/home.html>).

## REFERENCES

1. Tingle SJ, Figueiredo RS, Moir JA, et al. Machine perfusion preservation versus static cold storage for deceased donor kidney transplantation. *Cochrane Database Syst Rev.* 2019;3:CD011671.
2. Moers C, Smits JM, Maathuis MH, et al. Machine perfusion or cold storage in deceased-donor kidney transplantation. *N Engl J Med.* 2009;360:7–19.
3. Longchamp A, Mirabella T, Arduini A, et al. Amino acid restriction triggers angiogenesis via GCN2/ATF4 regulation of VEGF and H. *Cell.* 2018;173:117–129.e14.
4. Hine C, Kim HJ, Zhu Y, et al. Hypothalamic-pituitary axis regulates hydrogen sulfide production. *Cell Metab.* 2017;25:1320–1333.e5.
5. Bos EM, Wang R, Snijder PM, et al. Cystathionine γ-lyase protects against renal ischemia/reperfusion by modulating oxidative stress. *J Am Soc Nephrol.* 2013;24:759–770.
6. Hine C, Harputlugil E, Zhang Y, et al. Endogenous hydrogen sulfide production is essential for dietary restriction benefits. *Cell.* 2015;160:132–144.
7. Zhang MY, Dugbartey GJ, Juriasingani S, et al. Sodium thiosulfate-supplemented UW solution protects renal grafts against prolonged cold ischemia-reperfusion injury in a murine model of syngeneic kidney transplantation. *Biomed Pharmacother.* 2022;145:112435.
8. Sekijima M, Sahara H, Miki K, et al. Hydrogen sulfide prevents renal ischemia-reperfusion injury in CLAWN miniature swine. *J Surg Res.* 2017;219:165–172.
9. Juriasingani S, Jackson A, Zhang MY, et al. Evaluating the effects of subnormothermic perfusion with AP39 in a novel blood-free model of ex vivo kidney preservation and reperfusion. *Int J Mol Sci.* 2021;22:7180.

10. Macabrey D, Longchamp A, Déglise S, et al. Clinical use of hydrogen sulfide to protect against intimal hyperplasia. *Front Cardiovasc Med.* 2022;9:876639.
11. Corsello T, Komaravelli N, Casola A. Role of hydrogen sulfide in NRF2- and sirtuin-dependent maintenance of cellular redox balance. *Antioxidants (Basel).* 2018;7:129.
12. Chouchani ET, Pell VR, James AM, et al. A unifying mechanism for mitochondrial superoxide production during ischemia-reperfusion injury. *Cell Metab.* 2016;23:254–263.
13. Longchamp A, Klauser A, Songeon J, et al. Ex vivo analysis of kidney graft viability using 31P magnetic resonance imaging spectroscopy. *Transplantation.* 2020;104:1825–1831.
14. Szeto HH, Liu S, Soong Y, et al. Mitochondria-targeted peptide accelerates ATP recovery and reduces ischemic kidney injury. *J Am Soc Nephrol.* 2011;22:1041–1052.
15. Longchamp A, Meier RPH, Colucci N, et al. Impact of an intra-abdominal cooling device during open kidney transplantation in pigs. *Swiss Med Wkly.* 2019;149:w20143.
16. Agius T, Songeon J, Klauser A, et al. Subnormothermic ex vivo porcine kidney perfusion improves energy metabolism: analysis using. *Transplant Direct.* 2022;8:e1354.
17. Songeon J, Courvoisier S, Xin L, et al. In vivo magnetic resonance P-spectral analysis with neural networks: 31P-SPAWN. *Magn Reson Med.* 2023;89:40–53.
18. Meier RPH, Piller V, Hagen ME, et al. Intra-abdominal cooling system limits ischemia-reperfusion injury during robot-assisted renal transplantation. *Am J Transplant.* 2018;18:53–62.
19. Goujon JM, Hauet T, Menet E, et al. Histological evaluation of proximal tubule cell injury in isolated perfused pig kidneys exposed to cold ischemia. *J Surg Res.* 1999;82:228–233.
20. Lobb I, Davison M, Carter D, et al. Hydrogen sulfide treatment mitigates renal allograft ischemia-reperfusion injury during cold storage and improves early transplant kidney function and survival following allogeneic renal transplantation. *J Urol.* 2015;194:1806–1815.
21. Blackstone E, Morrison M, Roth MB. H<sub>2</sub>S induces a suspended animation-like state in mice. *Science.* 2005;308:518.
22. Blackstone E, Roth MB. Suspended animation-like state protects mice from lethal hypoxia. *Shock.* 2007;27:370–372.
23. Morrison ML, Blackwood JE, Lockett SL, et al. Surviving blood loss using hydrogen sulfide. *J Trauma.* 2008;65:183–188.
24. Haouzi P, Bell HJ, Notet V, et al. Comparison of the metabolic and ventilatory response to hypoxia and H<sub>2</sub>S in unsexed mice and rats. *Respir Physiol Neurobiol.* 2009;167:316–322.
25. Drabek T, Kochanek PM, Stezoski J, et al. Intravenous hydrogen sulfide does not induce hypothermia or improve survival from hemorrhagic shock in pigs. *Shock.* 2011;35:67–73.
26. Derwall M, Francis RC, Kida K, et al. Administration of hydrogen sulfide via extracorporeal membrane lung ventilation in sheep with partial cardiopulmonary bypass perfusion: a proof of concept study on metabolic and vasomotor effects. *Crit Care.* 2011;15:R51.
27. Chouchani ET, Pell VR, Gaude E, et al. Ischaemic accumulation of succinate controls reperfusion injury through mitochondrial ROS. *Nature.* 2014;515:431–435.
28. Asfar P, Calzia E, Radermacher P. Is pharmacological, H<sub>2</sub>S-induced 'suspended animation' feasible in the ICU? *Crit Care.* 2014;18:215.
29. Yu L, Di W, Dong X, et al. Dialllyl trisulfide exerts cardioprotection against myocardial ischemia-reperfusion injury in diabetic state, role of AMPK-mediated AKT/GSK-3β/HIF-1α activation. *Oncotarget.* 2017;8:74791–74805.
30. Li L, Whiteman M, Guan YY, et al. Characterization of a novel, water-soluble hydrogen sulfide-releasing molecule (GYY4137): new insights into the biology of hydrogen sulfide. *Circulation.* 2008;117:2351–2360.
31. Zhao H, Qiu Y, Wu Y, et al. Protective effects of GYY4137 on renal ischaemia/reperfusion injury through Nrf2-mediated antioxidant defence. *Kidney Blood Press Res.* 2021;46:257–265.
32. Ahmad A, Olah G, Szczesny B, et al. AP39, a mitochondrially targeted hydrogen sulfide donor, exerts protective effects in renal epithelial cells subjected to oxidative stress in vitro and in acute renal injury in vivo. *Shock.* 2016;45:88–97.
33. Urbanellis P, McEvoy CM, Škrtić M, et al. Transcriptome analysis of kidney grafts subjected to normothermic ex vivo perfusion demonstrates an enrichment of mitochondrial metabolism genes. *Transplant Direct.* 2021;7:e719.
34. Lam F, Li Y, Guo R, et al. Ultrafast magnetic resonance spectroscopic imaging using SPICE with learned subspaces. *Magn Reson Med.* 2020;83:377–390.
35. Lee HH, Kim H. Deep learning-based target metabolite isolation and big data-driven measurement uncertainty estimation in proton magnetic resonance spectroscopy of the brain. *Magn Reson Med.* 2020;84:1689–1706.